Multigraph-Based Curvilinear Regression Analysis of Two Novel Class of Drugs to Treat Cardiovascular Disease using Revan Indices

Ugasini Preetha P, M Suresh*

Abstract—**In this research, two distinct categories of medications for treating cardiovascular conditions, specifically fibrates and calcium channel blockers were analyzed. QSPR analysis of curvilinear regression models was used to establish a relationship between these degree-based indices and the physicochemical properties of some novel drugs used in the treatment of heart disease. The results show that quadratic regression outperformed linear regression for both drug classes. Additionally, comparing multigraph and simple graph modeling revealed that multigraph modeling provides a more detailed understanding of drug structures, enhancing the accuracy of estimating physicochemical properties. Specifically, eight Revan indices showed a strong correlation (R=1) in quadratic regression for fibrate drugs with the first Revan index (R_1) serving as the most accurate estimator for molar refractivity and polarizability. Meanwhile, the Geometric-Arithmetic Revan index (GAR) emerged as the best estimator for polar surface area in quadratic regression equations for calcium channel blockers. These studies highlight the potential of topological indices in estimating physicochemical properties of drugs, which could be useful in the development of new drugs and therapies.**

Index Terms—**Fibrates, calcium channel blockers, Revan topological indices, molecular multigraph, QSPR modeling, physicochemical properties.**

I. Introduction

Topological indices are valuable molecular descriptors for QSPR (Quantitative Structure-Property Relationship) modeling in chemistry, nanotechnology, and pharmacology, as they concisely capture structural and electronic properties of molecules.

Pharmacology has witnessed significant advancements, leading to the annual discovery of groundbreaking drugs. However, precise drug testing requires access to suitable equipment, a robust research network, and ample resources. The correlation between a drug's physical/chemical properties and molecular arrangement is well-established, making topological indices (TI's) a valuable tool for researchers in pharmacology and medicine to study molecular properties and their impact on experimental results [1],[2],[3],[4] and [5]. TI's can estimate the physicochemical properties of molecules, providing a cost-effective alternative to expensive laboratory experiments for developing nations.

In this study, we aim to explore the distinct characteristics of fibrates drugs and calcium channel blocking cardiac drugs. Fibrates are known for their ability to lower triglycerides, modestly affect LDL cholesterol levels, and raise HDL cholesterol levels, some common fibrate medications include Fenofibrate, Ciprofibrate, Bezafibrate and Clofibrate [6] and [7]. On the other side, calcium channel blockers are primarily used to treat hypertension, angina and abnormal heart rhythms by relaxing the heart's vessels and lowering blood pressure, some important calcium channel-blocking cardiac drugs include Nifedipine, Amlodipine, Diltiazem, Verapamil and ranolazine [8].

Chemical graph theory is an interdisciplinary field that combines mathematical modeling techniques with graph theory to understand chemical phenomena. [9], [10] and [11]. Topological indices (TI's) are important in this field, as they can be used to estimate molecular structural properties in QSAR/QSPR models. The Wiener index [12] introduced in 1947, was a pioneering TI that helped determine the physical properties of paraffin, marking a significant milestone in employing TI's for estimating and comprehending molecular characteristics. A fundamental understanding of molecular structure is crucial in the design of drugs as it aids in evaluating a compound's potential therapeutic benefits and overall efficacy. This knowledge enables researchers to make informed decisions, leading to improved drug design and enhanced therapeutic outcomes. The wealth of information encoded in molecular structure indices significantly contributes to understanding and predicting various characteristics and behaviors of chemical compounds [13], [14], [15] and [16]. The articles [17], [18], [19] and [20] provide valuable insights into the chemical, biological, and physical properties of diverse drugs/compounds through topological indices (TI's), enhancing the comprehensive QSAR/QSPR analysis of these substances.

This article focuses on the application of Revan indices in QSPR analysis, particularly in the context of drug discovery and design. Revan indices, initially introduced by V.R. Kulli [21], offer a robust framework for exploring the quantitative structure-property relationships of compounds, revealing non-linear patterns. The Revan vertex degree encompasses various indices, such as first and second Revan indices, modified first and second Revan indices, first and second

Manuscript received February 8, 2024; revised August 27, 2024.

Ugasini Preetha P is a Research scholar in Department of Mathematics, College of Engineering and Technology, SRM Institute of Science and Technology, Kattankulathur 603203, Tamil Nadu, India (e-mail: up4755@srmist.edu.in).

M. Suresh is an Assistant Professor in Department of Mathematics, College of Engineering and Technology, SRM Institute of Science and Technology, Kattankulathur - 603203, Tamilnadu, India. (corresponding author; e-mail: sureshm@srmist.edu.in).

hyper Revan indices, product connectivity Revan index, sum connectivity Revan index, harmonic Revan index, atom-bond connectivity Revan index, geometric-arithmetic Revan index, F-Revan index, and symmetric division Revan index [21],[22][23],[24],[25],[26] and [27]. In recent times, numerous researchers have been investigating various Topological Indices (TI's) across different drug classes like antiviral, anticancer, COVID-19, anti-tuberculosis, and asthma medications [28] [29] and [30]. Their aim is to develop Quantitative Structure-Property Relationship (QSPR) models using linear, quadratic, and cubic regression analyses to establish relationships between drug properties and their corresponding TI's. A recent study by Havare [31], utilized curvilinear regression models in a QSPR analysis focused on COVID-19 drugs. The study revealed that cubic regression models provide the most accurate estimation of properties for antiviral medications used in treating COVID-19 patients. Additionally, a limited number of studies, have explored the use of topological indices for analyzing specific drugs within the fibrates and calcium channel blockers drugs family [32], [33] and [34]. The Revan indices, along with their mathematical expressions, are detailed in Table I.

A multigraph is a graph theory concept that extends the idea of a simple graph allowing multiple edges between any pair of vertices [35]. In the book "Medicinal Chemistry: A Series of Monographs," Kier et al. [36] discuss Randic's argument that representing double bonds as double bonds provides a nuanced depiction of chemical structures. They compared a class of diene molecules as multigraphs and simple graphs concerning the boiling point property, finding that multigraphs slightly outperformed simple graph representations.

In this study, multigraph modeling is employed as a graph-based machine learning method to estimate drug physicochemical properties by representing drug structures as multigraphs, allowing for comprehensive capture of various chemical bonds and functional groups. Here, we employ curvilinear regression models to analyze the activity of fibrate and calcium channel blocker drugs based on their properties and topological indices (TI's). By integrating non-linear connections between variables, our objective is to enhance the accuracy and estimating capability of QSPR models in the analysis of these two distinct class of cardiac drugs. We focus on exploring the significance and applicability of various Revan topological indices as descriptors for chemical structures. The study is structured as follows: section 2 details the materials and methods employed, section 3 focuses on the main results, section 4 depicts model implementation and experimental results, section 5 shows further analysis to find the optimal estimators and section 6 summarizes the findings and their implications.

A. Motivation:

Our research, inspired by prior studies highlighting double bonds could improve correlation results in molecular modeling. Inspired by previous research such as that by Kier et al.'s [36] observation in "Medicinal Chemistry: A Series of Monographs" about double-edge counts providing a more accurate representation of double bonds. Recent work by Simon et al. also indicated improved correlations for molecules with weighted Wiener indices compared to traditional Wiener indices for simple graphs, while Zakharov et al. proposed a novel approach using multigraphs for enhanced statistical QSAR model building [37] and [38].

Inspired by these insights, we conducted a comparative analysis between simple and complex models to investigate the impact of double bonds on property estimation accuracy. Notably, no previous literature directly compares multigraph and simple graph efficacy in this context, making this study's contribution novel and original.

B. Notation:

Consider a connected graph $\mathcal{G}$, characterized by its vertex set $V(\mathcal{G})$ and edge set $E(\mathcal{G})$. The degree of a vertex 'x' in $\mathcal{G}$, denoted as $d_{\mathcal{G}}(x)$, indicates the number of neighboring vertices connected to 'x'. The maximum degree of $\mathcal{G}$ is represented as $\Delta_{max}(\mathcal{G})$, while the minimum degree is denoted as $\delta_{min}(\mathcal{G})$. In the context of Revan vertex degree, for a vertex 'x' belonging to $\mathcal{G}$, $r_{\mathcal{G}}(x) = \Delta_{max}(\mathcal{G}) + \delta_{min}(\mathcal{G}) - d_{\mathcal{G}}(x)$. Furthermore, the Revan edge 'xy' signifies the connection between the Revan vertices 'x' and 'y'.

TABLE I: Various Revan TI's: Mathematical Formulations

Vertex Degree Based Revan TI's	Mathematical Expression
First Revan index ($R_1(\mathcal{G})$)	$\sum_{xy\in E(\mathcal{G})}[r_{\mathcal{G}}(x) + r_{\mathcal{G}}(y)]$
Second Revan index ($R_2(\mathcal{G})$)	$\sum_{xy\in E(\mathcal{G})}[r_{\mathcal{G}}(x) \times r_{\mathcal{G}}(y)]$
First hyper Revan index ($HR_1(\mathcal{G})$)	$\sum_{xy\in E(\mathcal{G})}[r_{\mathcal{G}}(x) + r_{\mathcal{G}}(y)]^2$
Second hyper Revan index ($HR_2(\mathcal{G})$)	$\sum_{xy\in E(\mathcal{G})}[r_{\mathcal{G}}(x) \times r_{\mathcal{G}}(y)]^2$
1^{st} modified Revan index ($mR_1(\mathcal{G})$)	$\sum_{xy\in E(\mathcal{G})} \frac{1}{r_{\mathcal{G}}(x)+r_{\mathcal{G}}(y)}$
2^{nd} modified Revan index ($mR_2(\mathcal{G})$)	$\sum_{xy\in E(\mathcal{G})} \frac{1}{r_{\mathcal{G}}(x)\times r_{\mathcal{G}}(y)}$
Sum connectivity Revan index ($SR(\mathcal{G})$)	$\sum_{xy\in E(\mathcal{G})} \frac{1}{\sqrt{r_{\mathcal{G}}(x)+r_{\mathcal{G}}(y)}}$
Product connectivity Revan index ($PR(\mathcal{G})$)	$\sum_{xy\in E(\mathcal{G})} \frac{1}{\sqrt{r_{\mathcal{G}}(x)\times r_{\mathcal{G}}(y)}}$
F-Revan index ($FR(\mathcal{G})$)	$\sum_{xy\in E(\mathcal{G})}[r_{\mathcal{G}}(x)^2 + r_{\mathcal{G}}(y)^2]$
Atom-bond connectivity index ($ABC(\mathcal{G})$)	$\sum_{xy\in E(\mathcal{G})} \sqrt{\frac{r_{\mathcal{G}}(x)+r_{\mathcal{G}}(y)-2}{r_{\mathcal{G}}(x)\times r_{\mathcal{G}}(y)}}$
Geometric-arithmetic Revan index ($GAR(\mathcal{G})$)	$\sum_{xy\in E(\mathcal{G})} 2\sqrt{\frac{r_{\mathcal{G}}(x)\times r_{\mathcal{G}}(y)-2}{r_{\mathcal{G}}(x)+r_{\mathcal{G}}(y)}}$
Harmonic Revan index ($HR(\mathcal{G})$)	$\sum_{xy\in E(\mathcal{G})} \frac{2}{r_{\mathcal{G}}(x)+r_{\mathcal{G}}(y)}$
Symmetric division Revan index ($SDR(\mathcal{G})$)	$\sum_{xy\in E(\mathcal{G})} \left(\frac{r_{\mathcal{G}}(x)}{r_{\mathcal{G}}(y)} + \frac{r_{\mathcal{G}}(y)}{r_{\mathcal{G}}(x)}\right)$

II. Material and Method

This study investigates the physicochemical properties of fibrates and calcium channel blocker drugs, specifically Fenofibrate, Clofibrate, Bezafibrate, Ciprofibrate, Nifedipine, Amlodipine, Ailtiazem, Verapamil, and Ranolazine to gain insights into their structure-property relationships. Thirteen Revan TI's were used to model the chemical structures and SPSS statistical software version 25 was used to analyze the data. The study focused on four physicochemical properties for fibrates (polarizability(P), heat capacity(CV), octanol-water partition coefficients($XLogP_3$) and complexity(C)) and six properties for calcium channel blockers (boiling point(BP), enthalpy of vaporization(E), molar refractivity(MR), polar surface area(PSA), polarizability(P) and molar volume(MV)).

Linear equation :

$$D = a + bI; \qquad n, F, R, R^2, S.E, F - sig \qquad (1)$$

Quadratic equation :

$$D = a + b_1 I + b_2 I^2; \qquad n, F, R, R^2, S.E, F - sig \qquad (2)$$

In this particular context, the variable that reflects the response or dependence is identified as D, while the constant of the regression model is represented by the symbol "a." The individual descriptors' coefficients are symbolized as b_i (where i = 1, 2, 3), whereas the independent variable is represented as I. The regression equation is constructed using n samples. In the linear and quadratic regression analysis, statistical parameters with the highest correlation coefficient (R^2) value, minimal standard error (S.E), maximum (R) value, maximum F-value and F-sig with a p-value less than 0.05 were considered as indicators of the goodness of fit. These factors determine the quality of the regression models. The chemical structures of fibrates and calcium channel blocker drugs are depicted in Figure 1, which were drawn using ChemSketch software. Table II and Table XXXV (since this Table is large, it is placed before reference section) present the experimental values associated with these drugs and these values are taken from [32, 34].

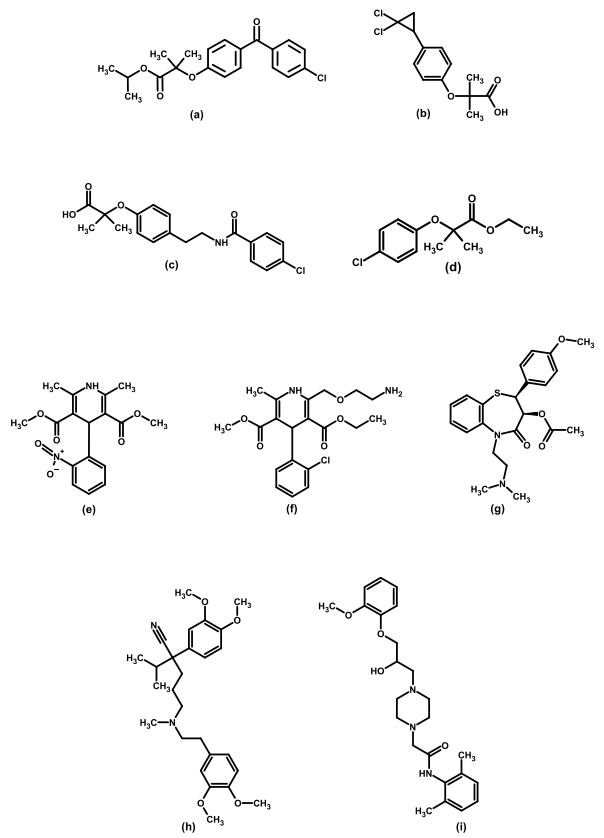

Fig. 1: Chemical Structures of Fibrates and Calcium Channel Blocker Drugs (a) Fenofibrate (b) Ciprofibrate (c) Bezafibrate (d) Clofibrate (e) Nifedipine (f) Amlodipine (g) Diltiazem (h) Verapamil (i) Ranolazine.

TABLE II: Physicochemical Characteristics of Investigated Fibrate Drugs

Fibrate Drugs	P	CV	$\mathbf{XLogP_3}$	C
Fenofibrate($\mathcal{F}$)	164.27567	66.502	5.2	458
Ciprofibrate ($\mathcal{C}$)	244.49533	92.538	3.4	333
Bezafibrate ($\mathcal{B}$)	232.43367	91.009	3.8	452
Clofibrate ($\mathcal{CL}$)	144.46	61.172	3.3	232

This research involves performing linear and quadratic regression models to estimate ten physicochemical properties using thirteen Revan TI's of nine cardiac drugs. Tables XXXVI (since this Table is large, it is placed before reference section), IV, and V display the Revan TI values and correlation coefficients from linear regression and correlation coefficients from quadratic regression, respectively of fibrate drugs. The regression model with the highest correlation coefficient is considered the most optimal estimator. The results from both linear and quadratic regression models for the physicochemical properties of fibrate drugs are presented in Tables VI, VII, VIII, IX, and X. Additionally, Figures 4 and 5 visually represent the optimal estimates of the linear and quadratic regression equations for the most precise physicochemical properties estimated by the Revan degree-based TI's.

III. Main Results

A. Evaluation of Fibrate Class of Cardiac Drugs: Multigraph Modeling versus Simple Graph Modeling

In this subsection, the computational analysis of the fibrate drugs involves studying its molecular structure through multigraph representation. The molecular multigraph of Fenofibrate is depicted in Figure 2. By using the Revan edge partition method, various Revan indices for Fenofibrate are calculated. Table III shows the Revan edge partitioning of Fenofibrate.

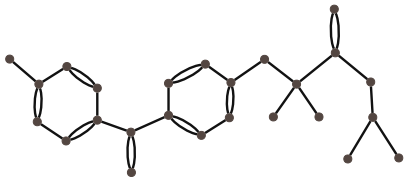

Fig. 2: Molecular Multigraph of Fenofibrate Drug

Theorem 1. *Let $\mathcal{F}$ be the molecular multigraph of Fenofibrate. Then we have,*

1) $R_1(\mathcal{F}) = 126$
2) $R_2(\mathcal{F}) = 106$
3) $HR_1(\mathcal{F}) = 500$
4) $HR_2(\mathcal{F}) = 422$
5) $mR_1(\mathcal{F}) = 9.8833$
6) $mR_2(\mathcal{F}) = 14$
7) $SR(\mathcal{F}) = 18.1549$
8) $PR(\mathcal{F}) = 21.1421$
9) $FR(\mathcal{F}) = 288$

10) $ABCR(\mathcal{F}) = 23.1628$
11) $GAR(\mathcal{F}) = 31.6413$
12) $HR(\mathcal{F}) = 19.7667$
13) $SDR(\mathcal{F}) = 91.25$

Proof: By using the mathematical equations of Revan indices as outlined in Table I, we have computed these indices as follows which provides a detailed account of the calculated indices and their significance in our analysis. Now by using Table III and by using Table I we get the following:

TABLE III: Revan Edge Partitioning for the Molecular Multigraph of Fenofibrate

$\mathbf{r_{\mathcal{G}}(x), r_{\mathcal{G}}(y)/xy \in E(\mathcal{G})}$	**Edge Count**
$(4,2)$	2
$(4,1)$	3
$(3,2)$	1
$(3,1)$	7
$(2,2)$	6
$(2,1)$	12
$(1,1)$	3

$$\begin{aligned} R_1(\mathcal{F}) &= \sum_{xy\in E(\mathcal{F})} [r_{\mathcal{F}}(x) + r_{\mathcal{F}}(y)] \\ &= 2(4+2) + 3(4+1) + (3+2) + 7(3+1) \\ &+ 6(2+2) + 12(2+1) + 3(1+1) \\ &= 126. \end{aligned}$$

$$\begin{aligned} R_2(\mathcal{F}) &= \sum_{xy\in E(\mathcal{F})} [r_{\mathcal{F}}(x) \times r_{\mathcal{F}}(y)] \\ &= 2(4\times 2) + 3(4\times 1) + (3\times 2) + 7(3\times 1) \\ &+ 6(2\times 2) + 12(2\times 1) + 3(1\times 1) \\ &= 106. \end{aligned}$$

$$\begin{aligned} HR_1(\mathcal{F}) &= \sum_{xy\in E(\mathcal{F})} [r_{\mathcal{F}}(x) + r_{\mathcal{F}}(y)]^2 \\ &= 2(4+2)^2 + 3(4+1)^2 + (3+2)^2 + 7(3+1)^2 \\ &+ 6(2+2)^2 + 12(2+1)^2 + 3(1+1)^2 \\ &= 500. \end{aligned}$$

$$\begin{aligned} HR_2(\mathcal{F}) &= \sum_{xy\in E(\mathcal{F})} [r_{\mathcal{F}}(x) \times r_{\mathcal{F}}(y)]^2 \\ &= 2(4\times 2)^2 + 3(4\times 1)^2 + (3\times 2)^2 + 7(3\times 1)^2 \\ &+ 6(2\times 2)^2 + 12(2\times 1)^2 + 3(1\times 1)^2 \\ &= 422. \end{aligned}$$

$$\begin{aligned} mR_1(\mathcal{F}) &= \sum_{xy\in E(\mathcal{F})} 1/[r_{\mathcal{F}}(x) + r_{\mathcal{F}}(y)] \\ &= 2(1/6) + 3(1/5) + (1/5) + 7(1/4) + 6(1/4) \\ &+ 12(1/3) + 3(1/2) \\ &= 9.8833 \end{aligned}$$

$$\begin{aligned} mR_2(\mathcal{F}) &= \sum_{xy\in E(\mathcal{F})} 1/[r_{\mathcal{F}}(x) \times r_{\mathcal{F}}(y)] \\ &= 2(1/8) + 3(1/4) + (1/6) + 7(1/3) \\ &+ 6(1/4) + 12(1/2) + 3(1/1) \\ &= 14 \end{aligned}$$

$$\begin{aligned} SR(\mathcal{F}) &= \sum_{xy\in E(\mathcal{F})} 1/\sqrt{r_{\mathcal{F}}(x) + r_{\mathcal{F}}(y)} \\ &= 2(1/\sqrt{6}) + 3(1/\sqrt{5}) + (1/\sqrt{5}) + 7(1/\sqrt{4}) \\ &+ 6(1/\sqrt{4}) + 12(1/\sqrt{3}) + 3(1/\sqrt{2}) \\ &= 18.1549 \end{aligned}$$

$$\begin{aligned} PR(\mathcal{F}) &= \sum_{xy\in E(\mathcal{F})} 1/\sqrt{r_{\mathcal{F}}(x) \times r_{\mathcal{F}}(y)} \\ &= 2(1/\sqrt{8}) + 3(1/\sqrt{4}) + (1/\sqrt{6}) + 7(1/\sqrt{3}) \\ &+ 6(1/\sqrt{4}) + 12(1/\sqrt{2}) + 3(1/\sqrt{1}) \\ &= 21.1421 \end{aligned}$$

$$\begin{aligned} FR(\mathcal{F}) &= \sum_{xy\in E(\mathcal{F})} [r_{\mathcal{F}}(x)^2 + r_{\mathcal{F}}(y)^2] \\ &= 2(16+4) + 3(16+1) + (9+4) + 7(9+1) \\ &+ 6(4+4) + 12(4+1) + 3(1+1) \\ &= 288. \end{aligned}$$

$$\begin{aligned} ABC(\mathcal{F}) &= \sum_{xy\in E(\mathcal{F})} \sqrt{\frac{r_{\mathcal{F}}(x) + r_{\mathcal{F}}(y) - 2}{r_{\mathcal{F}}(x) \times r_{\mathcal{F}}(y)}} \\ &= 2\sqrt{4/8} + 3\sqrt{3/4} + \sqrt{3/6} + 7\sqrt{2/3} \\ &+ 6\sqrt{2/4} + 12\sqrt{1/2} + 3\sqrt{0/1} \\ &= 23.1628 \end{aligned}$$

$$\begin{aligned} HR(\mathcal{F}) &= \sum_{xy\in E(\mathcal{F})} 2/[r_{\mathcal{F}}(x) + r_{\mathcal{F}}(y)] \\ &= 2(2/6) + 3(2/5) + (2/5) + 7(2/4) + 6(2/4) \\ &+ 12(2/3) + 3(2/2) \\ &= 19.7667. \end{aligned}$$

$$\begin{aligned} SDR(\mathcal{F}) &= \sum_{xy\in E(\mathcal{F})} \frac{r_{\mathcal{F}}(x)}{r_{\mathcal{F}}(y)} + \frac{r_{\mathcal{F}}(y)}{r_{\mathcal{F}}(x)} \\ &= 2(4/2 + 2/4) + 3(4/1 + 1/4) + (3/2 + 2/3) \\ &+ 7(3/1 + 1/3) + 6(2/2 + 2/2) \\ &+ 12(2/1 + 1/2) + 3(1/1 + 1/1) \\ &= 91.25. \end{aligned}$$

■

Following the same methodology as Theorem 1, the Revan indices for other drugs are also calculated and presented in Table XXXVI.

For simplicity, we have used the abbreviations $\mathcal{F}$, $\mathcal{C}$, $\mathcal{B}$, and $\mathcal{CL}$ to represent Fenofibrate, Ciprofibrate, Bezafibrate, and Clofibrate, respectively.

To illustrate the relationship between these properties and fibrate drugs modeled as simple graph, linear and quadratic regression analysis was performed using SPSS statistics 25. The simple graph representation of these fibrate drugs showed a linear regression correlation of *P with r = 0.575, CV with r = 0.558 and* $XLogP_3$ *with r = 0.744*. However, when modeled as molecular multigraphs of fibrates using linear regression, the correlation coefficients were significantly higher, as shown in Table IV. Similarly, for quadratic regression, the correlation coefficients were even higher as shown in Table V compared to to the simple graph modeling with *P having an 'r' value of 0.995, CV with r = 0.987,* $XLogP_3$ *with r = 0.986, and C with a perfect correlation coefficient of 1.*

From *Figure* 3 we observe that the high correlation coefficients 'r' values for physicochemical properties like polarizability (P), heat capacity (CV), octanol-water partition $(XLogP_3)$ and complexity (C) are higher in molecular multigraphs compared to simple graph representations of fibrate drugs. These findings demonstrate the potential of using molecular multigraphs which can provide a more detailed and nuanced representation of the chemical structure.

TABLE IV: Linear Regression: Correlation Coefficients (R) between Revan TI's and Physicochemical Properties for Molecular Multigraphs of Fibrates.

Revan TI	P	CV	$XLogP_3$
R_1	0.121	0.142	0.736
R_2	0.149	0.115	0.689
HR_1	0.012	0.017	0.707
HR_2	**0.642**	**0.593**	0.273
mR_1	0.198	0.209	0.777
mR_2	0.226	0.233	**0.785**
SR	0.195	0.208	0.765
PR	0.226	0.237	0.765
FR	0.1	0.125	0.709
$ABCR$	0.274	0.29	0.696
GAR	0.146	0.162	0.764
HR	0.198	0.209	0.777
SDR	0.174	0.193	0.725

TABLE V: Quadratic Regression: Correlation Coefficients (R) between Revan TI's and Physicochemical Properties for Molecular Multigraphs of Fibrates

Revan TI	P	CV	$XLogP_3$	C
R_1	0.496	0.445	0.795	0.996
R_2	0.916	0.889	0.697	0.985
HR_1	**0.996**	**0.988**	0.742	0.954
HR_2	0.645	0.599	**0.996**	0.794
mR_1	0.923	0.895	0.816	**1**
mR_2	0.945	0.921	0.85	**1**
SR	0.882	0.849	0.784	**1**
PR	0.892	0.861	0.798	**1**
FR	0.353	0.416	0.990	0.943
$ABCR$	0.613	0.57	0.708	**1**
GAR	0.875	0.841	0.773	**1**
HR	0.923	0.895	0.816	**1**
SDR	0.576	0.528	0.755	**1**

1) Remark: Correlation coefficients between the physicochemical properties and Revan topological Indices (TI's) were found to have identical correlation coefficients, it suggests that the strength and direction of their linear relationship are the same. Consequently, the same correlation coefficient values are are underlined and listed for these properties in both Tables IV and V.

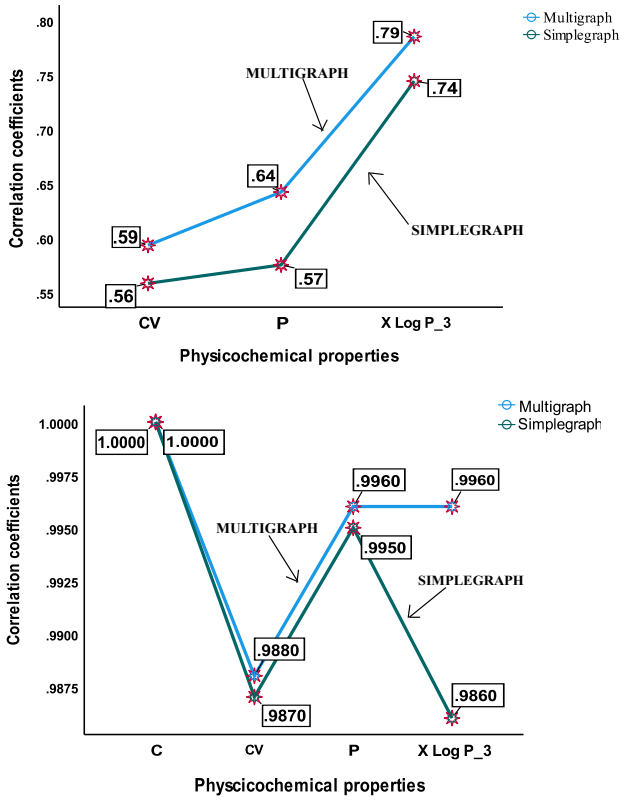

Fig. 3: Comparison Chart of 'r' values for Multigraph vs. Simple Graph using Linear and Quadratic Regression

Table VI highlights the optimal Revan TI values for estimating physicochemical properties of fibrate chemical structures using linear regression models. The table features bolded values that correspond to the highest coefficient of determination (R^2) for both multigraph and simple graph representations. These values signify the maximum level of accuracy achieved by the models and are accompanied by statistical parameters that evaluate the model's quality.

Figure 4 presents a visual representation of the information depicted in the above mentioned tables.

The highest coefficient of determination (R^2) for multigraph is greater than that for the simple graph, indicating that the multigraph models have a stronger fit. An F-value is used in ANOVA to assess overall model fit, with an F-value greater than 1 indicating significance. A higher F-value suggests a stronger fit, showing that independent variables collectively influence the dependent variable. All multigraph models have F-values above 1 compared to simple graph models.

However, some linear regression models in the simple

graph representations, such as for polarizability (P) and heat capacity, have F-values below 1, indicating that the models are not significant.

Additionally, lower standard errors in multigraph models indicate more precise and reliable regression models, demonstrating a better fit between observed and estimated data compared to simple graph models.

When comparing linear and quadratic regression models on multigraphs and simple graphs, quadratic models outperform in meeting statistical criteria. Statistical evaluation reveals that quadratic regression models on multigraph modeling show better adherence to criteria compared to those on simple graph modeling.

Tables VII, VIII, IX and X highlight the highest coefficient of determination (R^2) for both multigraph and simple graph models, with the quadratic models on multigraphs consistently exhibiting higher R^2 values.

TABLE VI: Optimal Linear Regression Models for the Physicochemical Properties

Linear Regression Model of Multigraph	$\mathbf{R^2}$	**F-Value**	**Sig**	**S.E**
$\mathbf{P = 320.646 - 0.318(HR_2)}$	**0.413**	**1.406**	**0.358**	**46.429**
$\mathbf{CV = 115.548 - 0.097(HR_2)}$	**0.351**	**1.084**	**0.407**	**16.065**
$\mathbf{XLogP_3 = 1.907 + 0.189(mR_2)}$	**0.616**	**3.204**	**0.215**	**0.666**
Linear Regression Model for Simple graph	$\mathbf{R^2}$	**F-Value**	**Sig**	**S.E**
$\mathbf{P = 47.530 + 35.644(mR_2)}$	**0.330**	**0.986**	**0.425**	**49.585**
$\mathbf{CV = 30.199 + 11.397(mR_2)}$	**0.311**	**0.904**	**0.442**	**16.553**
$\mathbf{XLogP_3 = 1.029 + 0.298(SR)}$	**0.554**	**2.486**	**0.256**	**0.717**

TABLE VII: Optimal Quadratic Regression Models for the Physicochemical Property Polarizability (P)

Quadratic Regression Model of Multigraph	$\mathbf{R^2}$	**F-Value**	**Sig**	**S.E**
$\mathbf{P = 6506.743 - 29.829(HR_1) + 0.034(HR_1^2)}$	**0.992**	**61.769**	**0.090**	**7.678**
$P = -607.689 + 167.76(mR_2) - 7.923(mR_2^2)$	0.893	4.190	0.327	27.975
$P = -1023.669 + 341.028(mR_1) - 22.126(mR_1^2)$	0.852	2.878	0.385	32.963
$P = -1023.696 + 170.517(HR) - 5.523(HR^2)$	0.852	2.878	0.385	32.963
$P = 2663.442 - 56.260(R_2) + 0.311(R_2^2)$	0.838	2.594	0.402	34.447
Quadratic Regression Model of Simple graph	$\mathbf{R^2}$	**F-Value**	**Sig**	**S.E**
$\mathbf{P = 1328.804 - 2.656(HR_2) + 0.001(HR_2^2)}$	**0.990**	**47.356**	**0.102**	**8.758**
$P = -2438.439 + 1395.488(mR_2) - 178.199(mR_2^2)$	0.931	6.753	0.263	22.497
$P = 4312.062 - 65.173(R_2) + 0.243(R_2^2)$	0.858	3.034	0.376	32.231

TABLE VIII: Optimal Quadratic Regression Models for the Physicochemical Property Heat Capacity (CV)

Quadratic Regression Model of Multigraph	$\mathbf{R^2}$	**F-Value**	**Sig**	**S.E**
$\mathbf{CV = 2137.139 - 9.741(HR_1) + 0.011(HR_1^2)}$	**0.977**	**21.351**	**0.151**	**4.267**
$CV = -179.893 + 53.533(mR_2) - 2.533(mR_2^2)$	0.848	2.797	0.389	10.985
Quadratic Regression Model of Simple graph	$\mathbf{R^2}$	**F-Value**	**Sig**	**S.E**
$\mathbf{CV = 446.751 - 0.868(HR_2) + 0.000(HR_2^2)}$	**0.974**	**19.060**	**0.160**	**4.510**
$CV = 1461.153 - 21.919(R_2) + 0.082(R_2^2)$	0.900	4.493	0.316	8.927
$CV = -774.661 + 451.662(mR_2) - 57.694(mR_2^2)$	0.892	4.148	0.328	9.252

TABLE IX: Optimal Quadratic Regression Models for the Physicochemical Property Octanol-Water Partition ($XLogP_3$)

Quadratic Regression Model of Multigraph	$\mathbf{R^2}$	**F-Value**	**Sig**	**S.E**
$\mathbf{XLogP_3 = -32.775 + 0.230(HR_2) + 0.000(HR_2^2)}$	**0.992**	**64.689**	**0.088**	**0.133**
$XLogP_3 = -142.121 + 1.170(FR) - 0.002(FR^2)$	0.980	25.049	0.140	0.213
Quadratic Regression Model of Simple graph	$\mathbf{R^2}$	**F-Value**	**Sig**	**S.E**
$\mathbf{XLogP_3 = -86.308 + 0.319(HR_1) + 0.000(HR_1^2)}$	**0.972**	**17.460**	**0.167**	**0.253**
$XLogP_3 = 43.141 - 22.318(mR_2) + 3.013(mR_2^2)$	0.922	5.945	0.297	0.423

TABLE X: Optimal Quadratic Regression Models for the Physicochemical Property Complexity (C)

Quadratic Regression Model of Multigraph	$\mathbf{R^2}$	**F-Value**	**Sig**	**S.E**
$C = -476.921 + 186.387(mR_1) - 9.311(mR_1^2)$	1	1420.465	0.019	3.503
$\mathbf{C = -179.537 + 79.376(mR_2) - 2.412(mR_2^2)}$	**1**	**6972.923**	**0.008**	**1.581**
$C = -719.951 + 132.450(SR) - 3.731(SR^2)$	1	822.218	0.025	4.604
$C = -382.850 + 73.788(PR) - 1.613(PR^2)$	1	2489.249	0.014	2.646
$C = -876.252 + 110.178(ABCR) - 2.278(ABCR^2)$	1	437.402	0.034	6.310
$C = -1655.480 + 150.778(GAR) - 2.659(GAR^2)$	1	392.304	0.036	6.663
$C = -476.958 + 93.199(HR) - 2.328(HR^2)$	1	1419.802	0.019	3.504
$C = -1593.616 + 50.346(SDR) - 0.305(SDR^2)$	1	410.794	0.035	6.511
Quadratic Regression Model of Simple graph	$\mathbf{R^2}$	**F-Value**	**Sig**	**S.E**
$C = -2274.171 + 45.690(R_1) - 0.189(R_1^2)$	1	1606.513	0.018	3.294
$C = -81.844 + 91.202(mR_1) + 2.564(mR_1^2)$	1	2377.267	0.015	2.708
$C = -407.954 + 115.219(SR) - 3.499(SR^2)$	1	4354.921	0.011	2.001
$C = 164.602 - 18.085(PR) + 4.172(PR^2)$	1	615.877	0.028	3.027
$C = -447.574 + 75.680(ABCR) - 1.460(ABCR^2)$	1	1902.898	0.016	3.027
$C = -487.158 + 67.853(GAR) - 1.206(GAR^2)$	1	839.448	0.024	4.556
$C = -81.784 + 45.586(HR) + 0.642(HR^2)$	1	2369.316	0.015	2.713
$\mathbf{C = 310.080 - 9.746(SDR) + 0.193(SDR^2)}$	**1**	**24307.296**	**0.005**	**0.847**

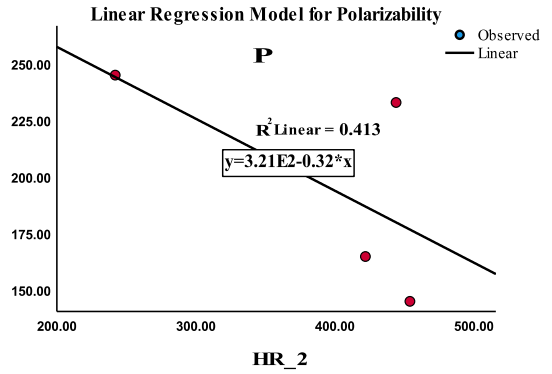

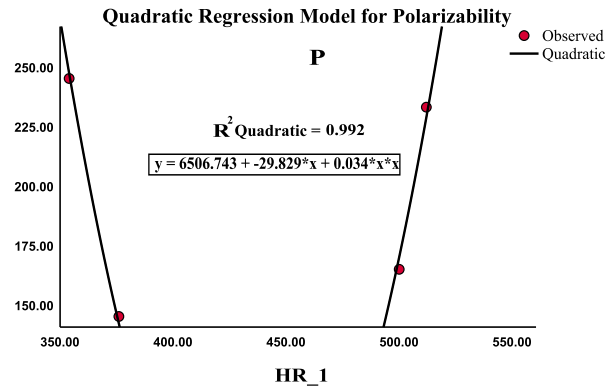

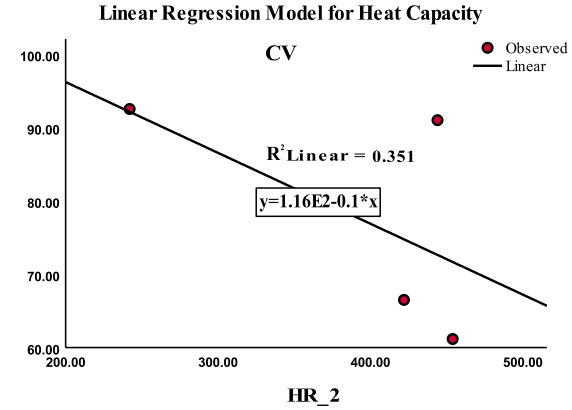

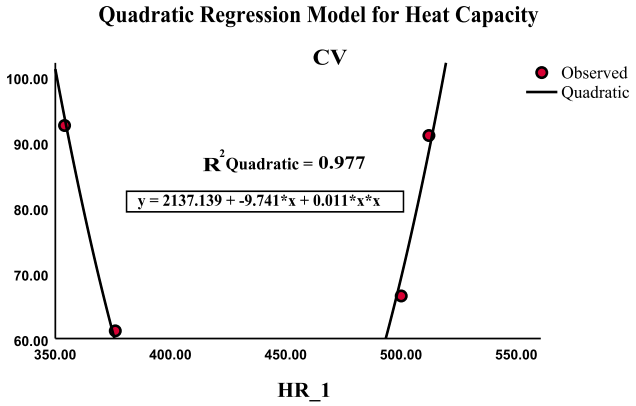

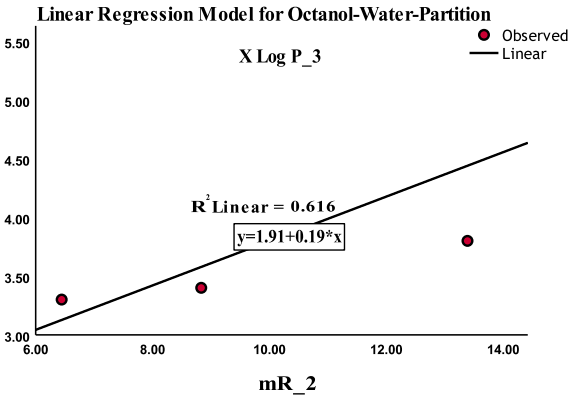

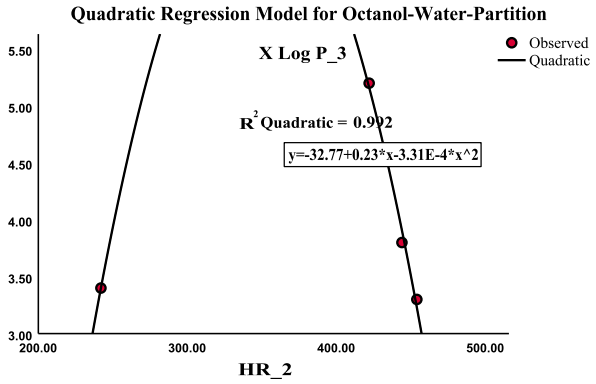

Fig. 4: Plots of Linear Regression Equation for the Good Estimates of the Selected Physicochemical Properties

Figure 5 shows the plots of quadratic regression equation for the good estimates in the above mentioned tables.

Notably, the physicochemical property ”complexity (C)” shows identical R^2 values of 1 for quadratic models of multigraph and simple graph modeling.

Overall, quadratic regression models on multigraphs demonstrate superior performance in modeling various physicochemical properties compared to simple graph models.

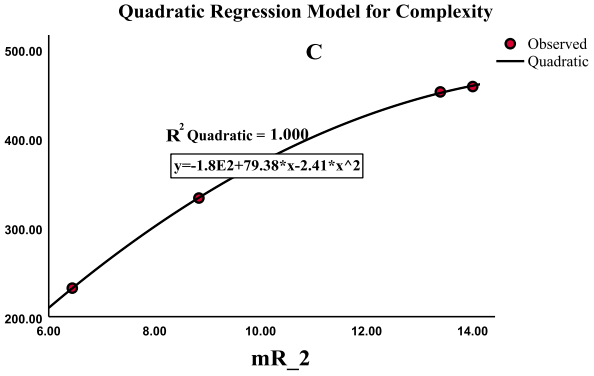

Fig. 5: Plots of Quadratic Regression Equation for the Good Estimates of the Selected Physicochemical Properties

B. Evaluation of Calcium Channel Blocker Class of Cardiac Drugs: Multigraph Modeling versus Simple graph Modeling

In this subsection, the computational analysis of medications that block calcium channels such as Nifedipine, Amlodipine, Diltiazem, Verapamil and Ranolazine which are used to treat heart conditions, this involves studying its molecular structure through multigraph representation. The molecular multigraph of Nifedipine is depicted in Figure 6. We analyzed the drugs' molecular structures and utilized computational methods to calculate Revan topological indices, by edge partitioning method. Table XI shows the Revan edge partitioning of Nifedipine. We analyzed the QSPR analysis of calculated indices and computed using linear and quadratic regression models with SPSS software.

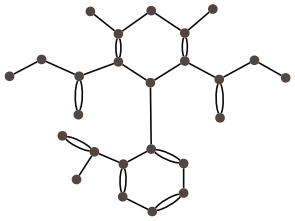

Fig. 6: Molecular Multigraph of Nifedipine Drug

Theorem 2. *Let $\mathcal{N}$ be the molecular multigraph of Nifedipine . Then,*

1) $R_1(\mathcal{N}) = 122$
2) $R_2(\mathcal{N}) = 104$
3) $HR_1(\mathcal{N}) = 492$
4) $HR_2(\mathcal{N}) = 526$
5) $mR_1(\mathcal{N}) = 10.7190$
6) $mR_2(\mathcal{N}) = 16.75$
7) $SR(\mathcal{N}) = 18.7959$
8) $PR(\mathcal{N}) = 22.8006$
9) $FR(\mathcal{N}) = 284$
10) $ABCR(\mathcal{N}) = 19.8322$
11) $GAR(\mathcal{N}) = 31.6394$
12) $HR(\mathcal{N}) = 21.4381$
13) $SDR(\mathcal{N}) = 91.75$

Proof: The initial molecule we are discussing is Nifedipine, following the same proof methodology as Theorem 1, we calculated for other drugs as well. For simplicity, we have used the abbreviations $\mathcal{N}$, $\mathcal{A}$, $\mathcal{D}$, $\mathcal{V}$ and $\mathcal{R}$ to represent Nifedipine, Amlodipine, Diltiazem, Verapamil and Ranolazine respectively. The multigraph representation of Nifedipine is shown in Figure 6, it has 25 vertices and 34 edges. Now, we will obtain the following by Revan topological index values using Table I and edge partition Table XI.

TABLE XI: Revan Edge Partitioning for the Molecular Multigraph of Nifedipine.

$\mathbf{r_G(x)}, \mathbf{r_G(y)}/\mathbf{xy} \in \mathbf{E}(\mathcal{G})$	**Edge Count**
$(4,3)$	2
$(4,1)$	3
$(3,1)$	10
$(2,2)$	4
$(2,1)$	7
$(1,1)$	8

The obtained values for topological indices of the Nifedipine and other drugs are shown in Table XXXVII (since this Table is large, it is placed before reference section).

■

DISCUSSION:

The physicochemical characteristics of calcium channel blocker medications used in heart disease treatment are detailed in Table XXXV as mentioned. Additionally, Table XII illustrates the correlation coefficient (R) between the Revan topological indices and the drugs' physicochemical properties using linear regression equations. The highest R value highlighted in bold, signifies the significance of all features with a p-value below 0.05. Furthermore, Table XIII showcases the optimal linear regression equations for estimating the physical and chemical attributes of these drugs, emphasizing the maximum R and R-squared value, minimum SE value and maximum F value.

Table XIV displays the correlation coefficient (R) derived from quadratic regression equations, with the highest value marked in bold. In Table XV, quadratic regression equations are presented to best approximate the physical and chemical features of the drugs under investigation. The R_1 and GAR indices exhibit the strongest correlation coefficient (R) with the MR, P and PSA characteristics, with a coefficient of 1 in quadratic equations. Based on criteria such as max(R), min(SE) and max(F), R_1 and GAR indices emerge as the most accurate estimators for MR, P and PSA in the quadratic models.

In comparison to Hasani and Ghods' research cited in [34], our research shows superior regression models (both linear and quadratic) for estimating specific physicochemical properties of the drugs being analyzed. However, when considering linear regression models, the drugs represented as multigraphs demonstrate slightly lower correlation coefficients (R) for certain properties like BP, E, PSA and MV, with a difference of around 5-10% compared to Hasani and Ghods' simpler graph representation of the drugs. For quadratic regression models, our multigraph modeling shows better correlation results compared to Hasani and Ghods' simple graph modeling of the drugs under study. Notably, the physicochemical characteristics MR and P exhibits correlation coefficient R = 1 compared to the simple graph modeling with the coefficient of R = 0.989 and also for other physicochemical characteristics our models performed slightly better than Hasani and Ghods'.

TABLE XII: The Correlation Coefficient (R) of Multigraph Modeling Calculated by Linear Regression Models

	BP	E	MR	PSA	P	MV
$\mathbf{R_1}$	0.352	0.326	0.788	0.805	0.787	**0.913**
$\mathbf{R_2}$	0.262	0.228	0.723	0.74	0.722	0.876
$\mathbf{HR_1}$	0.255	0.222	0.718	0.736	0.717	0.873
$\mathbf{HR_2}$	0.187	0.152	0.666	0.686	0.665	0.838
$\mathbf{mR_1}$	0.165	0.125	0.65	0.668	0.649	0.821
$\mathbf{mR_2}$	0.356	0.327	0.792	0.81	0.792	0.897
SR	0.124	0.179	0.388	0.407	0.386	0.633
PR	0.186	0.146	0.665	0.683	0.664	0.834
FR	0.248	0.217	0.713	0.732	0.712	0.869
ABCR	0.789	0.806	0.861	0.867	0.862	0.67
GAR	**0.837**	0.853	**0.99**	**0.994**	**0.989**	0.902
HR	0.165	0.125	0.65	0.668	0.649	0.821
SDR	0.78	**0.874**	0.882	0.919	0.882	0.703

TABLE XIII: The Most Optimal Estimators for Certain Physicochemical Properties using Linear Regression Equations

Regression Equations: Our Results using Multigraph Modeling					
Equation	**R**	$\mathbf{R^2}$	**F**	**SE**	**p-value**
MR = -75.916 + 5.232(GAR)	0.99	0.979	142.518	2.788	0.001
P = -30.293 + 2.080(GAR)	0.989	0.979	139.979	1.118	0.001
Regression Equations: Hasani and Ghods' [34]					
MR = -73.026 + 2.640(SDD)	0.987	0.974	112.506	3.13	0.001
P = -29.128 + 1.049(SDD)	0.987	0.973	109.115	1.263	0.001

TABLE XIV: The Correlation Coefficient (R) of Multigraph Modeling Calculated by Quadratic Regression Models

	BP	E	MR	PSA	P	MV
$\mathbf{R_1}$	0.989	0.962	**1**	0.984	**1**	0.984
$\mathbf{R_2}$	**0.991**	0.919	0.985	0.952	0.985	**0.998**
$\mathbf{HR_1}$	0.988	0.926	0.985	0.955	0.985	**0.998**
$\mathbf{HR_2}$	0.863	0.677	0.878	0.822	0.878	0.979
$\mathbf{mR_1}$	0.317	0.145	0.662	0.669	0.662	0.823
$\mathbf{mR_2}$	0.911	0.888	0.965	0.959	0.966	0.932
SR	0.866	**0.979**	0.958	0.994	0.958	0.934
PR	0.822	0.526	0.852	0.78	0.853	0.932
FR	0.984	0.933	0.984	0.957	0.984	**0.998**
ABCR	0.968	0.928	0.955	0.929	0.956	0.826
GAR	0.976	0.899	**0.99**	**1**	**0.99**	0.922
HR	0.318	0.145	0.662	0.669	0.662	0.823
SDR	0.78	0.874	0.882	0.919	0.882	0.703

As we notice that in Table XIV, the physicochemical characteristic MV has three different optimal estimators (R_1, HR_1 and FR) with the same coefficient $R = 0.998$ which means that when the same correlation coefficient is obtained with different estimators in estimating a physicochemical property, it implies that the estimators have similar accuracy in estimating the property. However, this does not necessarily mean that the estimators are equally good. The choice of the best estimator may depend on other factors such as coefficient of determination (R-squared) or the root mean to evaluate the performance of the estimators. For MV, based on R-squared and other statistical measures R_1 index stands as the optimal estimator.

Tables XVI and XVII demonstrate a close match between the estimated values of the optimal estimators' physicochemical features of drugs, confirming the accuracy of these descriptors. The R_1 and GAR indices is identified as the most accurate estimators for MR, P and PSA attributes in quadratic regression equations, with a correlation coefficient of R = 1.

TABLE XV: The Most Optimal Estimators for Certain Physicochemical Properties using Quadratic Regression Equations

Regression Equations: Our Results using Multigraph Modeling					
Equation	**R**	$\mathbf{R^2}$	**F**	**SE**	**p-value**
BP = 160.651 + 3.531(R_2) - 0.005(R_2^2)	0.991	0.981	52.06	10.964	0.019
E = 994.323 - 105.773(SR) + 3.025(SR^2)	0.979	0.958	22.704	2.57	0.042
MR = -82.613 + 1.849(R_1) - 0.004(R_1^2)	1	0.999	1748.041	0.569	<0.001
PSA = -96.839 + 16.486(GAR) - 0.315(GAR^2)	1	1	3229.734	0.466	<0.001
P = -33.069 + 0.736(R_1) - 0.001(R_1^2)	1	0.999	1444.355	0.249	<0.001
MV = 89.657 + 1.996(R_2) - 0.002(R_2^2)	0.998	0.997	289.83	4.767	0.003
Regression Equations: Hasani and Ghods' [34]					
BP = -5526.995 + 168.715(SDD) - 1.159(SDD^2)	0.974	0.949	18.573	18.052	0.051
E = -894.503 + 5.089(F) - 0.007(F^2)	0.931	0.866	6.473	4.577	0.134
MR = -282.958 + 8.707(SDD) - 0.044(SDD^2)	0.989	0.979	45.824	3.476	0.021
PSA = 116.929 + 2.185(SDD) - 0.037(SDD^2)	1	1	4128.059	0.412	<0.001
P = -116.047 + 3.561(SDD) - 0.018(SDD^2)	0.989	0.978	44.973	1.395	0.022
MV = 692.932 - 195.766(mM_2) + 21.355(mM_2^2)	0.998	0.996	246.814	5.164	0.004

TABLE XVI: Comparing Actual and Estimated Values using a Quadratic Regression Model for R_1 Index

Drugs	**MR**	$\mathbf{R_1}$	**P**	$\mathbf{R_1}$
Nifedipine	87.9 $\pm$ 0.3	**83.429**	34.8 $\pm$ 0.5	**41.839**
Amlodipine	105.4 $\pm$ 0.3	**99.289**	41.8 $\pm$ 0.5	**51.279**
Diltiazen	115.2 $\pm$ 0.4	**107.269**	45.7 $\pm$ 0.5	**56.559**
Verapamil	131.9 $\pm$ 0.3	**100.873**	52.3 $\pm$ 0.5	**99.855**
Ranolazine	122.1 $\pm$ 0.3	**114.097**	48.4 $\pm$ 0.5	**61.551**

TABLE XVII: Comparing Actual and Estimated Values using a Quadratic Regression Model for GAR Index

Drugs	**PSA (act.)**	**GAR (est.)**
Nifedipine	110	**109.4369**
Amlodipine	100	**99.72664**
Diltiazen	84	**82.88412**
Verapamil	64	**63.21052**
Ranolazine	74	**73.6657**

Figures 7, 8 and 9 illustrates the correlation of the R_1 index with MR, P and GAR index with PSA.

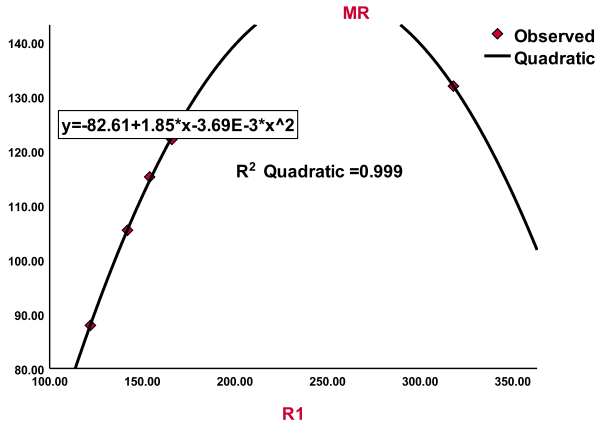

Fig. 7: Correlation R_1 Index with MR

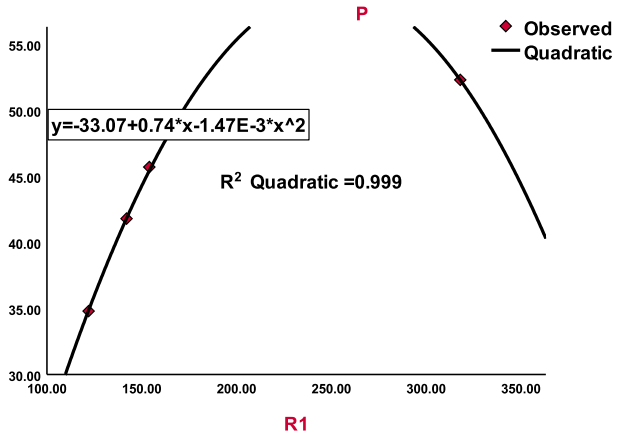

Fig. 8: Correlation R_1 Index with P

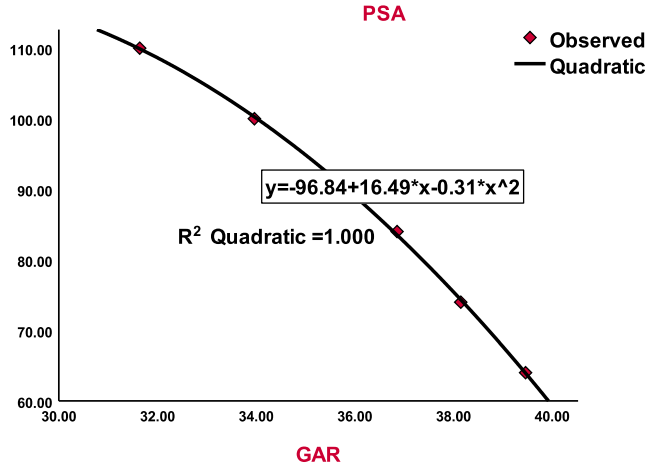

Fig. 9: Correlation GAR Index with PSA

IV. Model Implementation and Experimental Results

From Tables II,III,V and XIV we implement a linear and quadratic regression model using equations 1 and 2 to estimate the physicochemical properties of heart disease drugs. Tables XVIII - XXIV display the experimental results implemented from linear and quadratic regression model of fibrate drugs modeled as multigraphs and simple graphs. Tables XXV - XXXII display the experimental results implemented from linear and quadratic regression model of calcium channel blocker drugs modeled as multigraphs and simple graphs. These tables includes the predicted values from linear and quadratic regression models with their respective physicochemical property.

A. Evaluation of Model Performance

To evaluate the efficacy of the experimental results, we examine the performance metrics of linear and quadratic regression model as shown in Table XVIII to Table XXXII using root-mean-square deviation (RMSE). RMSE is the standard deviation of the residuals (prediction errors) in a regression model. It provides a measure of how concentrated the data points are around the regression line, with lower RMSE values indicating a better fit. The effectiveness of a model is determined by its ability to demonstrate lower RMSE values for each physicochemical property. The statistics was calculated by the following equation:

$$RMSE = \sqrt{\frac{1}{N}\sum_{1}^{N}(I_{obs,k} - I_{pred,k})^2} \tag{3}$$

where N is the number of the sample size and $I_{obs,k}$ and $I_{pred,k}$ are the observed and predicted physicochemical properties for each sample i, respectively.

TABLE XVIII: Observed, Predicted and RMSE value of Fibrate Drugs for the Physicochemical Property Polarizability

Linear Regression Model of Multigraph			
Fibrate Drugs	**P (Obs.)**	$\mathbf{HR_2(Pred.)}$	**RMSE**
Fenofibrate	164.2757	186.45	**11.0872**
Ciprofibrate	244.4953	243.69	
Benzafibrate	232.4337	179.454	
Clofibrate	144.46	176.274	
Linear Regression Model of Simple graph			
Fibrate Drugs	**P (Obs.)**	$\mathbf{mR_2(Pred.)}$	**RMSE**
Fenofibrate	164.2757	216.3435	**26.0339**
Ciprofibrate	244.4953	203.9680	
Benzafibrate	232.4337	210.8971	
Clofibrate	144.46	154.462	

TABLE XIX: Observed, Predicted and RMSE value of Fibrate Drugs for the Physicochemical Property Heat Capacity

Linear Regression Model of Multigraph			
Fibrate drugs	**CV (Obs.)**	$\mathbf{HR_2(Pred.)}$	**RMSE**
Fenofibrate	66.502	74.614	**4.056**
Ciprofibrate	92.538	92.074	
Benzafibrate	91.009	72.48	
Clofibrate	61.172	71.51	
Linear Regression Model of Simple graph			
Fibrate drugs	**CV (Obs.)**	$\mathbf{mR_2(Pred.)}$	**RMSE**
Fenofibrate	66.502	84.1763	**8.8372**
Ciprofibrate	92.538	80.2193	
Benzafibrate	91.009	82.4349	
Clofibrate	61.172	64.39	

TABLE XX: Observed, Predicted and RMSE value of Fibrate Drugs for the Physicochemical Property Octanol- Water Partition

Linear Regression Model of Multigraph			
Fibrate drugs	**$XLogP_3$(Obs.)**	**mR_2(Pred.)**	**RMSE**
Fenofibrate	5.2	4.553	**0.3235**
Ciprofibrate	3.4	3.5765	
Benzafibrate	3.8	4.4375	
Clofibrate	3.3	3.1250	
Linear Regression Model of Simple graph			
Fibrate drugs	**$XLogP_3$(Obs.)**	**SR (Pred.)**	**RMSE**
Fenofibrate	5.2	4.4754892	**0.3623**
Ciprofibrate	3.4	3.6394204	
Benzafibrate	3.8	4.4481328	
Clofibrate	3.3	3.1371414	

TABLE XXI: Observed, Predicted and RMSE value of Fibrate Drugs for the Physicochemical Property Polarizability

Quadratic Regression Model of Multigraph			
Fibrate drugs	**P (Obs.)**	**HR_1(Pred.)**	**RMSE**
Fenofibrate	164.2757	92.243	**36.0163**
Ciprofibrate	244.4953	208.021	
Benzafibrate	232.4337	147.191	
Clofibrate	144.46	97.823	
Quadratic Regression Model of Simple graph			
Fibrate drugs	**P (Obs.)**	**HR_2(Pred.)**	**RMSE**
Fenofibrate	164.2757	-390.259	**277.2673**
Ciprofibrate	244.4953	77.876	
Benzafibrate	232.4337	-418.139	
Clofibrate	144.46	-130.076	

TABLE XXII: Observed, Predicted and RMSE value of Fibrate Drugs for the Physicochemical Property Heat Capacity

Quadratic Regression Model of Multigraph			
Fibrate drugs	**CV (Obs.)**	**HR_1(Pred.)**	**RMSE**
Fenofibrate	66.502	16.639	**24.9315**
Ciprofibrate	92.538	67.301	
Benzafibrate	91.009	33.331	
Clofibrate	61.172	29.659	
Quadratic Regression Model of Simple graph			
Fibrate drugs	**CV (Obs.)**	**HR_2(Pred.)**	**RMSE**
Fenofibrate	66.502	-522.805	**294.6535**
Ciprofibrate	92.538	-84.465	
Benzafibrate	91.009	-593.981	
Clofibrate	61.172	-226.817	

TABLE XXIII: Observed, Predicted and RMSE value of Fibrate Drugs for the Physicochemical Property Octanol-Water Partition

Quadratic Regression Model of Multigraph			
Fibrate drugs	**$XLogP_3$(Obs.)**	**HR_2(Pred.)**	**RMSE**
Fenofibrate	5.2	64.285	**29.5425**
Ciprofibrate	3.4	22.885	
Benzafibrate	3.8	69.345	
Clofibrate	3.3	71.645	
Quadratic Regression Model of Simple graph			
Fibrate drugs	**$XLogP_3$(Obs.)**	**HR_1(Pred.)**	**RMSE**
Fenofibrate	5.2	138.906	**66.853**
Ciprofibrate	3.4	60.432	
Benzafibrate	3.8	145.286	
Clofibrate	3.3	58.518	

TABLE XXIV: Observed, Predicted and RMSE value of Fibrate Drugs for the Physicochemical Property Complexity

Quadratic Regression Model of Multigraph			
Fibrate drugs	**C (Obs.)**	**mR_2(Pred.)**	**RMSE**
Fenofibrate	458	458.975	**0.4875**
Ciprofibrate	333	333.4134	
Benzafibrate	452	450.8388	
Clofibrate	232	231.8226	
Quadratic Regression Model of Simple graph			
Fibrate drugs	**C (Obs.)**	**SDR (Pred.)**	**RMSE**
Fenofibrate	458	457.2636	**0.3682**
Ciprofibrate	333	332.1301	
Benzafibrate	452	450.0902	
Clofibrate	232	231.4462	

TABLE XXV: Observed, Predicted and RMSE value of Fibrate Drugs for the Physicochemical Property Molar Refractivity

Linear Regression Model of Multigraph			
Calcium blocker drugs	**MR (Obs.)**	**GAR (Pred.)**	**RMSE**
Nifedipine	87.9	89.6213	**0.7698**
Amlodipine	105.4	101.7789	
Diltiazen	115.2	116.9146	
Verapamil	131.9	130.5413	
Ranolazine	122.1	123.6696	
Linear Regression Model of Simple graph			
Calcium blocker drugs	**MR (Obs.)**	**SDD (Pred.)**	**RMSE**
Nifedipine	87.9	90.654	**2.4244** [34]
Amlodipine	105.4	101.214	
Diltiazen	115.2	115.2762	
Verapamil	131.9	131.3538	
Ranolazine	122.1	124.0938	

TABLE XXVI: Observed, Predicted and RMSE value of Fibrate Drugs for the Physicochemical Property Polarizability

Linear Regression Model of Multigraph			
Calcium blocker drugs	**P (Obs.)**	**GAR (Pred.)**	**RMSE**
Nifedipine	34.8	35.5170	**0.3206**
Amlodipine	41.8	40.3502	
Diltiazen	45.7	46.3675	
Verapamil	52.3	51.7848	
Ranolazine	48.4	49.0530	
Linear Regression Model of Simple graph			
Calcium blocker drugs	**P (Obs.)**	**SDD (Pred.)**	**RMSE**
Nifedipine	34.8	35.91	**0.9782** [34]
Amlodipine	41.8	40.106	
Diltiazen	45.7	45.6936	
Verapamil	52.3	52.0820	
Ranolazine	48.4	49.1973	

TABLE XXVII: Observed, Predicted and RMSE value of Fibrate Drugs for the Physicochemical Property Boiling Point

Quadratic Regression Model of Multigraph			
Calcium blocker drugs	**BP (Obs.)**	$\mathbf{R_2(Pred.)}$	**RMSE**
Nifedipine	475.3	473.795	
Amlodipine	572.2	565.435	
Diltiazen	594.4	571.663	**0.6731**
Verapamil	586.2	411.677	
Ranolazine	624.1	618.247	
Quadratic Regression Model of Simple graph			
Calcium blocker drugs	**BP (Obs.)**	**SDD (Pred.)**	**RMSE**
Nifedipine	475.3	478.139	
Amlodipine	572.2	559.591	
Diltiazen	594.4	610.4785	**9.2089** [34]
Verapamil	586.2	588.0773	
Ranolazine	624.1	608.8382	

TABLE XXVIII: Observed, Predicted and RMSE value of Fibrate Drugs for the Physicochemical Property Enthalpy

Quadratic Regression Model of Multigraph			
Calcium blocker drugs	**E (Obs.)**	**SR (Pred.)**	**RMSE**
Nifedipine	73.9	74.9140	
Amlodipine	80.2	78.1308	
Diltiazen	88.6	90.8744	**0.4535**
Verapamil	87.5	87.4361	
Ranolazine	97.2	95.5332	
Quadratic Regression Model of Simple graph			
Calcium blocker drugs	**E (Obs.)**	**F (Pred.)**	**RMSE**
Nifedipine	73.9	24.331	
Amlodipine	80.2	28.279	
Diltiazen	88.6	28.517	**2.8949** [34]
Verapamil	87.5	16.561	
Ranolazine	97.2	24.331	

TABLE XXIX: Observed, Predicted and RMSE value of Fibrate Drugs for the Physicochemical Property Molar Refractivity

Quadratic Regression Model of Multigraph			
Calcium blocker drugs	**MR (Obs.)**	$\mathbf{R_1(Pred.)}$	**RMSE**
Nifedipine	87.9	83.429	
Amlodipine	105.4	99.289	
Diltiazen	115.2	107.269	**1.9995**
Verapamil	131.9	100.873	
Ranolazine	122.1	114.097	
Quadratic Regression Model of Simple graph			
Calcium blocker drugs	**MR (Obs.)**	**SDD (Pred.)**	**RMSE**
Nifedipine	87.9	87.74	
Amlodipine	105.4	100.04	
Diltiazen	115.2	114.2334	**2.1982** [34]
Verapamil	131.9	127.4018	
Ranolazine	122.1	121.8596	

TABLE XXX: Observed, Predicted and RMSE value of Fibrate Drugs for the Physicochemical Property Polar Surface Area

Quadratic Regression Model of Multigraph			
Calcium blocker drugs	**PSA (Obs.)**	**GAR (Pred.)**	**RMSE**
Nifedipine	110	109.4369	
Amlodipine	100	99.7266	
Diltiazen	84	82.8841	**0.2518**
Verapamil	64	63.2105	
Ranolazine	74	73.6657	
Quadratic Regression Model of Simple graph			
Calcium blocker drugs	**PSA (Obs.)**	**SDD (Pred.)**	**RMSE**
Nifedipine	110	110.171	
Amlodipine	100	99.967	
Diltiazen	84	84.5407	**0.2607** [34]
Verapamil	64	64.3311	
Ranolazine	74	73.7968	

TABLE XXXI: Observed, Predicted and RMSE value of Fibrate Drugs for the Physicochemical Property Polarizability

Quadratic Regression Model of Multigraph			
Calcium blocker drugs	**P (Obs.)**	$\mathbf{R_1(Pred.)}$	**RMSE**
Nifedipine	34.8	41.839	
Amlodipine	41.8	51.279	
Diltiazen	45.7	56.559	**3.1479**
Verapamil	52.3	99.855	
Ranolazine	48.4	61.551	
Quadratic Regression Model of Simple graph			
Calcium blocker drugs	**P (Obs.)**	**SDD (Pred.)**	**RMSE**
Nifedipine	34.8	35.543	
Amlodipine	41.8	40.571	
Diltiazen	45.7	46.3723	**0.882** [34]
Verapamil	52.3	51.7536	
Ranolazine	48.4	49.4889	

TABLE XXXII: Observed, Predicted and RMSE value of Fibrate Drugs for the Physicochemical Property Molar Volume

Quadratic Regression Model of Multigraph			
Calcium blocker drugs	**MV (Obs.)**	$\mathbf{R_2(Pred.)}$	**RMSE**
Nifedipine	272.3	275.609	
Amlodipine	333	335.609	
Diltiazen	327.6	339.851	**1.4798**
Verapamil	429.4	555.401	
Ranolazine	364	372.491	
Quadratic Regression Model of Simple graph			
Calcium blocker drugs	**MV (Obs.)**	$\mathbf{mM_2(Pred.)}$	**RMSE**
Nifedipine	272.3	270.0209	
Amlodipine	333	330.0664	
Diltiazen	327.6	318.4768	**3.2659** [34]
Verapamil	429.4	421.983	
Ranolazine	364	364.065	

Our aim is to obtain a prediction using multigraph model that will perform better than the classical simple graph model

and also establish a relationship between the independent variable and dependent variable. We proceed to analyze the performance measurements of our models across multiple tables.

In Table XVIII, which represents a QSPR linear regression model of the HR_2, mR_2 and polarizability of fibrate drugs, the multigraph model exhibited lower RMSE values, indicating its superior performance over simple graph model. Similarly, in Table XIX, multigraph model achieved lower RMSE values. This suggests that multigraph outperformed simple graph in the QSPR linear regression model for HR_2, mR_2 indices and heat capacity of fibrate drugs.

Moving on to Table XX, multigraph model outperformed simple graph model in the QSPR linear regression model between mR_2, SR indices and octanol-water partition, exhibited lower RMSE values of 0.3235(multigraph) and 0.3623(simplegraph).

From Tables XXI, XXII, XXIII and XXIV, multigraph model with lower RMSE values consistently outperformed simple graph model in the QSPR quadratic regression for polarizability, heat capacity and octanol-water partition except for complexity, the simple graph model achieved lower RMSE value of 0.3682.

For the QSPR linear regression model of the indices GAR and SDD, Tables XXVI and XXVII indicates that our multigraph model with lower RMSE values outperformed Hasani and Ghods' [34] simple graph model with higher RMSE values in predicting the physicochemical properties molar refractivity and polarizability.

Lastly, from Tables XXVIII - XXXII demonstrates the superiority of our multigraph modeling over simple graph modeling of Hasani and Ghod's [34] in the QSPR quadratic regression model for the indices R_2, SDD, SR, F, R_1, GAR and the physicochemical properties boiling point, enthalpy, molar refractivity, polar surface area, polarizability and molar volume of calcium channel blocker cardiac drugs. Multigraph modeling obtained lower RMSE values for all physicochemical properties except polarizability.

The impact of lower RMSE suggests that the model's predictions are more accurate and the model's predicted values are on average closer to the actual values of the physicochemical properties, indicating that the model is better at estimating the relationship between the Revan indices and the corresponding physicochemical properties of cardiac drugs.

From Tables XXI - XXXV, there is a total of 30 linear and quadratic regression metric of physicochemical properties recorded for both the multigraph and simple graph modeling which is divided across 11 optimal Revan indices. The multigraph modeling obtained the lower RMSE values in 26 of the linear and quadratic regression metric of physicochemical properties recorded across the 11 optimal Revan indices while the simple graph modeling obtained lower RMSE value in only 4 of the linear and quadratic regression metric of physicochemical properties across 11 optimal Revan indices. From this, we confirm that the multigraph modeling is a better prediction model in QSPR analysis of the physicochemical properties of two novel class of cardiac drugs.

B. Graphical Performance Measure for Multigraph versus Simple graph

In this subsection, we present the comparative model plots for the best Revan estimators (TI's). The plot compares the QSPR linear and quadratic regression models with RMSE values between different Revan TI's of the multigraph and simple graph models for the physicochemical properties of two novel class of cardiac drugs. By comparing the RMSE value of simple graph and multigraph modeling 3D- clustered column chart, one can observe the differences in their RMSE values across the different physicochemical properties.

If the RMSE value of multigraph modeling's column height consistently stays below the simple graph modeling column height, it indicates that the multigraph model generally outperforms the simple graph model in terms of accuracy and predictive power for the physicochemical property. Conversely, if the simple graph modeling column height consistently stays below the multigraph modeling column height, it suggests that the simple graph modeling performed better. The following are plots (Figs. 10 - 13) that show the comparison between the RMSE of multigraph and simple graph models across best Revan estimators.

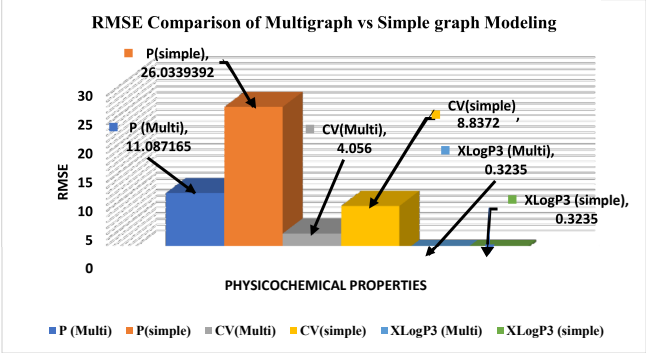

Fig. 10: RMSE Comparison in Linear Regression of Fibrate Drugs: Multigraph Vs. Simplegraph for P, CV and $XLogP_3$

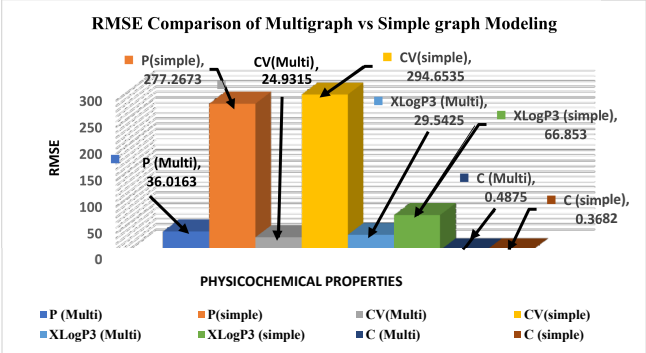

Fig. 11: RMSE Comparison in Quadratic Regression of Fibrate Drugs: Multigraph Vs. Simplegraph for P, CV, $XLogP_3$ and C

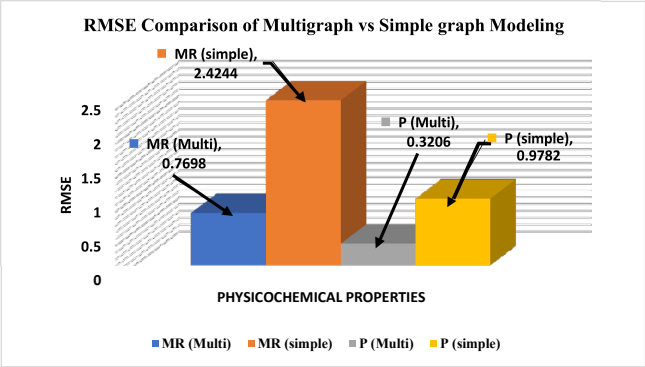

Fig. 12: RMSE Comparison in Linear Regression of Calcium Channel Blocker Drugs: Multigraph Vs. Simplegraph for MR and P

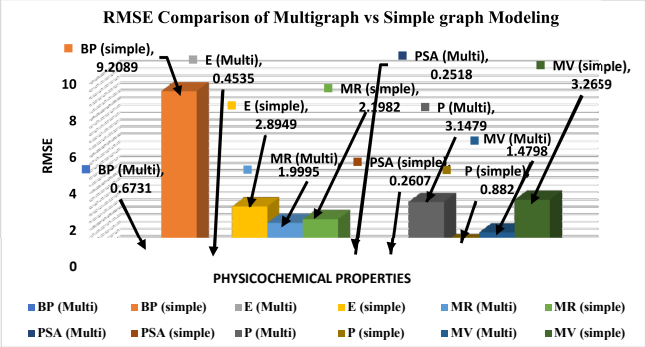

Fig. 13: RMSE Comparison in Quadratic Regression of Calcium Channel Blocker Drugs: Multigraph Vs. Simplegraph for BP, E, MR, PSA, P and MV

From the plots it is evident that the physicochemical properties where the optimal Revan TI's of multigraph modeling obtained a general superiority with its lower RMSE values, one can observe the major difference in Figures 11, followed by 12, 10 and 13. From the previous literature (see [34]), that the RMSE values obtained by simple graph modeling exhibited higher RMSE values and also exhibited lower correlations compared to our multigraph modeling in the QSPR analysis. However, the use of this approach has made it possible to achieve improvement in this regard, this is shown in the lower RMSE values recorded for all best estimators of Revan TI's except Table XXIV and XXIX in the multigraph model.

V. Further Analysis on the Estimators:

In this section, we have performed further analysis on the results of our previous section. Biplot confirmed the optimal estimators from quadratic regression of fibrates and calcium channel blockers. Principal Component Analysis (PCA) is a dimensionality reduction technique used to transform high-dimensional data into a lower-dimensional space, capturing the most significant variance in the data. It is often accompanied by a scree plot, which helps determine the number of principal components to retain and a biplot, which visually represents both the observations and variables in the reduced space for easier interpretation and analysis of relationships. From Table XXXIII and Figure 14, shows the eigenvalues associated with each principal component.

The data of this study underwent reduction employing the Kaiser criterion, resulting in two principal components chosen based on eigenvalues exceeding 1. These three components collectively account for 98.48 % of the system's variability.

TABLE XXXIII: Eigenvalues, Percent of Variance and Cumulative Derived from PCA

No. of PC's	Eigenvalues	Variance explained %	Cumulative
1	7.2383	55.68%	55.68%
2	5.5646	42.80%	98.48%

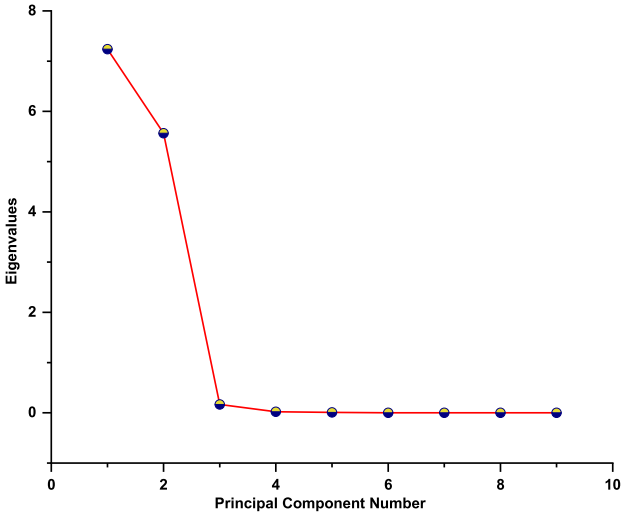

Fig. 14: Scree Plot of Eigenvalues of the PC's

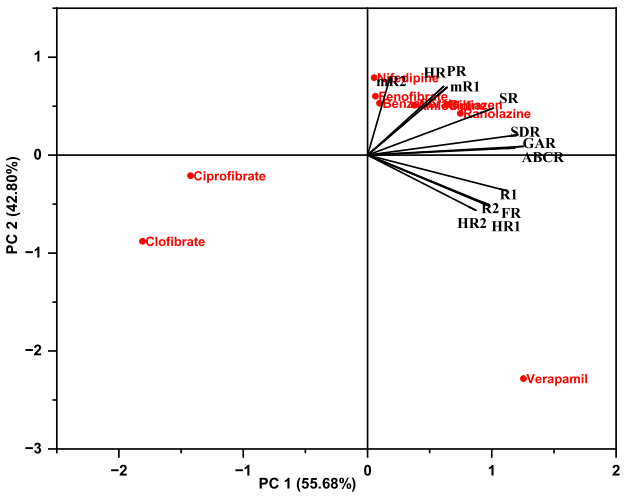

Fig. 15: Biplot of Eigenvalues of the PC's

Table XXXIV and Figure 15, shows the extracted eigen vectors representing estimators can help identify

TABLE XXXIV: Eigen Vectors Derived from PCA

Extracted Eigen Vectors		
$\mathbf{PC_1}$	$\mathbf{PC_2}$	
55.68%	**42.80%**	
0.33096	-0.19262	R_1
0.28754	-0.26689	R_2
0.28601	-0.26974	HR_1
0.25653	-0.29735	HR_2
0.18804	**0.36471**	mR_1
0.05329	**0.41694**	mR_2
0.29807	0.25312	SR
0.18013	**0.37034**	PR
0.28427	-0.27154	FR
0.34853	0.03786	ABCR
0.36918	0.04725	GAR
0.18803	**0.36478**	HR

which drugs with its physicochemical properties are most influential in predicting the drug's performance.

From biplot, we see that these drugs Ciprofibrate, Clofibrate and Verapamil are distant from others might have unique properties or different mechanisms of action but other drugs that are close to each other in the biplot share similar physicochemical properties. Now the projection of a drug onto a vector (estimators) shows how strongly that drug is associated with its physicochemical properties. Longer vectors indicate that the estimator has a stronger influence on the variability among the drugs. For example, we see from Table XXXIV the bolded values representing the longest eigen vectors form PC_1 and PC_2.

From these findings we see that this aligns with our quadratic regression results' optimal estimators of both class of cardiac drugs.

VI. Conclusion

In this study, we examined thirteen topological descriptors based on Revan edge partitioning using maximum degree, minimum degree and degree of that vertex for two novel class of distinct cardiac drugs named as fibrates and calcium channel blockers for treating heart disease: Fenofibrate, Ciprofibrate, Bezafibrate and Clofibrate, Nifedipine, Amlodipine, Diltiazem, Verapamil and Ranolazine. These drug structures are modeled as multigraphs to estimate the physicochemical properties of these drugs under study.

QSPR modeling has shown that the most effective topological descriptors for estimating the physical and chemical features for fibrate drugs are the HR_2 index for (P) and (CV), the mR_2 index for $XLogP_3$ in linear regression models.

Furthermore, in quadratic equations, the best estimators for physicochemical features are HR_1 index for (P) and (CV), HR_2 index for $XLogP_3$, for the physicochemical attribute complexity (C), eight estimators(topological descriptors) exhibits strong correlation value (R = 1) but among them we validated the best estimator with the statistical measures like coefficient of determination (R-squared), F-value, SE etc. which is mR_2 index.

Through extensive data analysis and experimentation, it has been demonstrated that multigraph model with lower RMSE values outperformed simple graph model in estimating the physicochemical properties of two novel class of cardiac drugs.

Additionally, among all the QSPR analyses conducted using Revan topological indices, molar volume (MV) in quadratic regression of calcium channel blocker drugs emerged as the physical property that achieved the lowest RMSE values for both the multigraph and simple graph models. Following polarizability, octanol-water partition and enthalpy also demonstrated relatively low RMSE values in the analyses.

From this, we conclude that the multigraph model is a better estimation model in QSPR analysis of the physicochemical properties of two novel class of cardiac drugs.

Similarly, the QSPR modeling for calcium channel blocking cardiac drugs in linear regression equations, the GAR index is the optimal estimator in estimating the physicochemical features (MR) and (P). For quadratic regression equations, the R_1 index for (MR) and (P), R_2 index for (BP) and (MV), SR index for (E) and GAR index for (PSA). Notably, two estimators R_1 and GAR shows strong correlation coefficient (R=1) and GAR index demonstrate a close match between the estimated values of the features and the real values, confirming the accuracy of these descriptors. The GAR index is identified as the most accurate estimator for (PSA).

The biplot analysis highlights that drugs such as Ciprofibrate, Clofibrate, and Verapamil exhibit distinct properties, while others cluster together, indicating similar characteristics. The strong influence of certain physicochemical properties, as evidenced by the prominent eigenvectors, aligns our quadratic regression findings, validating the key estimators for predicting drug performance.

This study highlights the importance of considering multigraphs as graph models, offering a novel perspective on drug connectivity analysis.

By diverging from conventional approaches focused on simple graphs, the research has provided insights into optimizing the drug selection process and researchers can advance our understanding of drug behavior and improve strategies for enhancing drug effectiveness.

TABLE XXXV: Physicochemical Characteristics of Investigated Calcium Channel Blocker Drugs

Calcium Channel Blocker Drugs	BP(°C)	E(kJ/mol)	MR(cm^3)	PSA(A^2)	P($10^{-24}cm^3$)	MV(cm^3)
Nifedipine ($\mathcal{N}$)	475.3 ± 45	73.9 ± 3	87.9 ± 0.3	110	34.8 ± 0.5	272.3 ± 3
Amlodipine ($\mathcal{A}$)	572.2 ± 50	80.2 ± 3	105.4 ± 0.3	100	41.8 ± 0.5	333 ± 3
Diltiazen ($\mathcal{D}$)	594.4 ± 50	88.6 ± 3	115.2 ± 0.4	84	45.7 ± 0.5	327.6 ± 5
Verapamil ($\mathcal{V}$)	586.2 ± 50	87.5 ± 3	131.9 ± 0.3	64	52.3 ± 0.5	429.4 ± 3
Ranolazine ($\mathcal{R}$)	624.1 ± 55	97.2 ± 3	122.1 ± 0.3	74	48.4 ± 0.5	364 ± 3

TABLE XXXVI: Values of Various Revan TI's Modeled as Molecular Multigraphs for Fibrate Drugs

Fibrate drugs	R_1	R_2	HR_1	HR_2	mR_1	mR_2	SR	PR	FR	ABCR	GAR	HR	SDR
Fenofibrate	126	106	500	422	9.8833	14	18.1549	21.1421	288	23.1628	31.6413	19.7667	91.25
Ciprofibrate	88	70	354	242	6.3667	8.8333	12.0092	13.9519	214	16.8979	20.8524	12.7333	60.0833
Bezafibrate	128	108	512	444	9.6333	13.3889	17.9478	20.7708	296	24.0573	31.4419	19.2667	93.6667
Clofibrate	84	82	376	454	5.1095	6.4444	10.0142	10.961	212	14.2473	18.6621	10.219	53.8333

TABLE XXXVII: Values of Various Revan TI's Modeled as Molecular Multigraphs for Calcium Channel Blocker Drugs

Calcium channel blocker drugs	R_1	R_2	HR_1	HR_2	mR_1	mR_2	SR	PR	FR	ABCR	GAR	HR	SDR
Nifedipine	122	104	492	526	10.719	16.75	18.7959	22.8006	284	19.8322	31.6394	21.4381	91.75
Amlodipine	142	144	640	968	10.5786	15.6944	19.1525	22.3453	352	21.4619	33.9631	21.1571	92.25
Diltiazen	154	147	652	761	10.5595	13.6944	20.1288	22.4031	358	27.6927	36.856	21.119	98.3333
Verapamil	318	626	2608	12014	5.6228	3.8728	15.0618	11.9255	1356	26.7116	39.4605	11.2455	98.4333
Ranolazine	166	171	748	987	10.7262	14.2083	20.4054	22.4852	406	25.6494	38.1471	21.4524	98.25

REFERENCES

[1] Estrada, E. and Uriarte, E., "Recent advances on the role of topological indices in drug discovery research", *Current Medicinal Chemistry*, vol. 8, no. 13, pp. 1573-1588, 2001.

[2] Gao, W., Farahani, M.R. and Shi, L., "Forgotten topological index of some drug structures", *Acta Medica Mediterranea*, vol. 32, no. 1, pp. 579-585, 2016.

[3] Gao, W., Wang, W. and Farahani, M.R., "Topological indices study of molecular structure in anticancer drugs", *Journal of Chemistry*, vol. 2016, no. 1, pp. 1-8, 2016.

[4] Gao, W., Wang, Y., Basavanagoud, B. and Jamil, M.K., "Characteristics studies of molecular structures in drugs", *Saudi Pharmaceutical Journal*, vol. 25, no. 4, pp. 580-586, 2017.

[5] Gonzalez-Diaz, H., Vilar, S., Santana, L. and Uriarte, E., "Medicinal chemistry and bioinformatics-current trends in drugs discovery with networks topological indices", *Current Topics in Medicinal Chemistry*, vol. 7, no. 10, pp. 1015-1029, 2007.

[6] Jun, M., Foote, C., Lv, J., Neal, B., Patel, A., Nicholls, S.J., Grobbee, D.E., Cass, A., Chalmers, J. and Perkovic, V., "Effects of fibrates on cardiovascular outcomes: a systematic review and meta-analysis", *The Lancet*, vol. 375, no. 9729, pp. 1875-1884, 2010.

[7] Staels, B., Dallongeville, J., Auwerx, J., Schoonjans, K., Leitersdorf, E. and Fruchart, J.C., "Mechanism of action of fibrates on lipid and lipoprotein metabolism", *Circulation Journal*, vol. 98, no. 19, pp. 2088-2093, 1998.

[8] Kelley, D., "Heart disease: Causes, prevention, and current research", *JCCC Honors Journal*, vol. 5, no. 2, pp. 1-15, 2014.

[9] Gutman, I., "Degree-based topological indices", *Croatica Chemica Acta*, vol. 86, no. 4, pp. 351-361, 2013.

[10] Hosoya, H., "Topological index. A newly proposed quantity characterizing the topological nature of structural isomers of saturated hydrocarbons", *Bulletin of the Chemical Society of Japan*, vol. 44, no. 9, pp. 2332-2339, 1971.

[11] Gutman, I., "A property of the simple topological index", *MATCH Communications in Mathematical and in Computer Chemistry*, vol. 25, pp. 131-140, 1990.

[12] Wiener, H., "Structural determination of paraffin boiling points", *Journal of the American Chemical Society*, vol. 69 no. 1, pp. 17-20, 1947.

[13] Samsonov, G.V., "Handbook of the Physicochemical Properties of the Elements", *Springer Science & Business Media*, 2012.

[14] Estrada, E., "Characterization of 3D molecular structure", *Chemical Physics Letters*, vol. 319, no. 5-6, pp. 713-718, 2000.

[15] Gutman, I. and Trinajstić, N., "Graph theory and molecular orbitals. Total π-electron energy of alternant hydrocarbons", *Chemical Physics Letters*, vol. 17, no. 4, pp. 535-538, 1972.

[16] Randic, M., "Characterization of molecular branching", *Journal of the American Chemical Society*, vol. 97, no. 23, pp. 6609-6615, 1975.

[17] Öztürk Sözen, E. and Eryaşar, E., "QSPR analysis of some drug candidates investigated for COVID-19 via new topological coindices", *Polycyclic Aromatic Compounds*, vol. 44, no. 2, pp. 1291-1308, 2024.

[18] Arockiaraj, M., Campena, F.J.H., Greeni, A.B., Ghani, M.U., Gajavalli, S., Tchier, F. and Jan, A.Z., "QSPR analysis of distance-based structural indices for drug compounds in tu-

berculosis treatment", *Heliyon*, vol. 10, no. 2, pp. e23981, 2024.
[19] Kirmani, S.A.K., Ali, P. and Azam, F., "Topological indices and QSPR/QSAR analysis of some antiviral drugs being investigated for the treatment of COVID-19 patients", *International Journal of Quantum Chemistry*, vol. 121, no. 9, pp. e26594, 2021.
[20] Mondal, S., Dey, A., De, N. and Pal, A., "QSPR analysis of some novel neighbourhood degree-based topological descriptors", *Complex & Intelligent Systems*, vol. 7, no. 2, pp. 977-996, 2021.
[21] Kulli, V.R., "On the product connectivity Revan index of certain nanotubes", *Journal of Computer and Mathematical Sciences*, vol. 8, no. 10, pp. 562-567, 2017.
[22] Kulli, V.R., "Revan indices of oxide and honeycomb networks", *International Journal of Mathematics and its Applications*, vol. 55, no. 4-E, pp. 663-667, 2017.
[23] Kulli, V.R., "The sum connectivity Revan index of silicate and hexagonal networks", *Annals of Pure and Applied Mathematics*, vol. 14, no. 3, pp. 401-406, 2017.
[24] Kulli, V.R., "Revan Polynomials of Chloroquine, Hydroxychloroquine, Remdesivir; Research for the Treatment of COVID-19", *SSRG International Journal of Applied Chemistry*, vol. 7, no. 2, pp. 6-12, 2020.
[25] Kulli, V.R., "F-Revan index and F-Revan polynomial of some families of benzenoid systems", *Journal of Global Research in Mathematical Archives*, vol. 5, no. 11, pp. 1-6, 2018.
[26] Kulli, V.R., "Hyper-Revan indices and their polynomials of silicate networks", *International Journal of Current Research in Science and Technology*, vol. 4, no. 3, pp. 17-21, 2018.
[27] Kulli, V.R., "K Banhatti polynomials of remdesivir, chloroquine and hydroxychloroquine: Research Advances for the prevention and treatment of COVID-19", *SSRG International Journal of Applied Chemistry*, vol. 7, no. 2, pp. 48-55, 2020.
[28] Havare, Ö.C., "Topological indices and QSPR modeling of some novel drugs used in the cancer treatment", *International Journal of Quantum Chemistry*, vol. 121, no. 24, pp. e26813, 2021.
[29] Ravi, Vignesh, and Kalyani Desikan., "Curvilinear regression analysis of benzenoid hydrocarbons and computation of some reduced reverse degree based topological indices for hyaluronic acid-paclitaxel conjugates", *Scientific Reports*, vol. 13, no. 1, pp. 3239, 2023.
[30] Tamilarasi, William, and Bommahalli Jayaraman Balamurugan., "QSPR Model Through Revan Indices to Predict Physicochemically and ADMET Properties of Anti-Flaviviral Drugs to Treat Zika Virus", *Biointerface Research in Applied Chemistry*, vol. 13, no. 6, pp. 556-569, 2023.
[31] Havare, O.C., "QSPR analysis with curvilinear regression modeling and topological indices", *Iranian Journal of Mathematical Chemistry*, vol. 10, no. 4, pp. 331-341, 2019.
[32] Delen, S., Khan, R.H., Kamran, M., Salamat, N., Baig, A.Q., Naci Cangul, I. and Pandit, M.K., "Ve-degree, ev-degree, and degree-based topological indices of fenofibrate", *Journal of Mathematics*, vol. 2022, no. 1, pp. 4477808, 2022.
[33] Wazzan, S. and Ozalan, N.U., "Exploring the Symmetry of Curvilinear Regression Models for Enhancing the Analysis of Fibrates Drug Activity through Molecular Descriptors", *Symmetry*, vol. 15, no. 6, 1160, pp. 1-22, 2023.
[34] Hasani, M. and Ghods, M., "Calculation of topological indices along with MATLAB coding in QSPR analysis of calcium channel-blocking cardiac drugs", *Journal of Mathematical Chemistry*, pp. 1-22, 2024.
[35] Trudeau, R.J., "Introduction to graph theory", *Courier Corporation*, 2013.
[36] Hite, G., "Diuretics: Chemistry and Pharmacology. Volume 1 of medicinal chemistry: A series of monographs", *Academic Press*, New York., 1964.
[37] Brezovnik, S., Tratnik, N. and Žigert Pleteršek, P., "Weighted Wiener indices of molecular graphs with application to alkenes and alkadienes", *Mathematics*, vol. 9, no. 2, 153, pp. 1-16, 2021.
[38] Zakharov, A.B., Tsarenko, D.K. and Ivanov, V.V., "Topological characteristics of iterated line graphs in the QSAR problem: A multigraph in the description of properties of unsaturated hydrocarbons", *Structural Chemistry*, vol. 32, no. 4, pp. 1629-1639, 2021.